

# **Supplementary Material**

## **The structure of amorphous and deeply supercooled liquid alumina**

**C. Shi<sup>1,2</sup>, O. L.G. Alderman<sup>3</sup>, D. Berman<sup>4</sup>, J. Du<sup>4</sup>, J. Neuefeind<sup>5</sup>, A. Tamalonis<sup>3</sup>,  
J. K. R. Weber<sup>2,3</sup>, J. You<sup>1</sup>, C. J. Benmore<sup>2</sup>**

1. State Key Laboratory of Advanced Special Steel, Shanghai Key Laboratory of Advanced Ferrometallurgy, School of Materials Science and Engineering, Shanghai University, Shanghai, China

2. X-Ray Science Division, Advanced Photon Source, Argonne National Laboratory, Argonne, Illinois, USA

3. Materials Development, Inc., Arlington Heights, Illinois, USA

4. Materials Science and Engineering, University of North Texas, Denton, Texas, USA.

5. Neutron Scattering Division, Oak Ridge National Laboratory, Oak Ridge, Tennessee, USA.

\* **Correspondence:** Dr. Chris Benmore: [benmore@anl.gov](mailto:benmore@anl.gov)

**Figure S1** plots a comparison of  $Q^*[S(Q)-1]$  measured in pure oxygen and argon, which reveals the atmosphere has a small effect on the structure of supercooled liquid alumina.

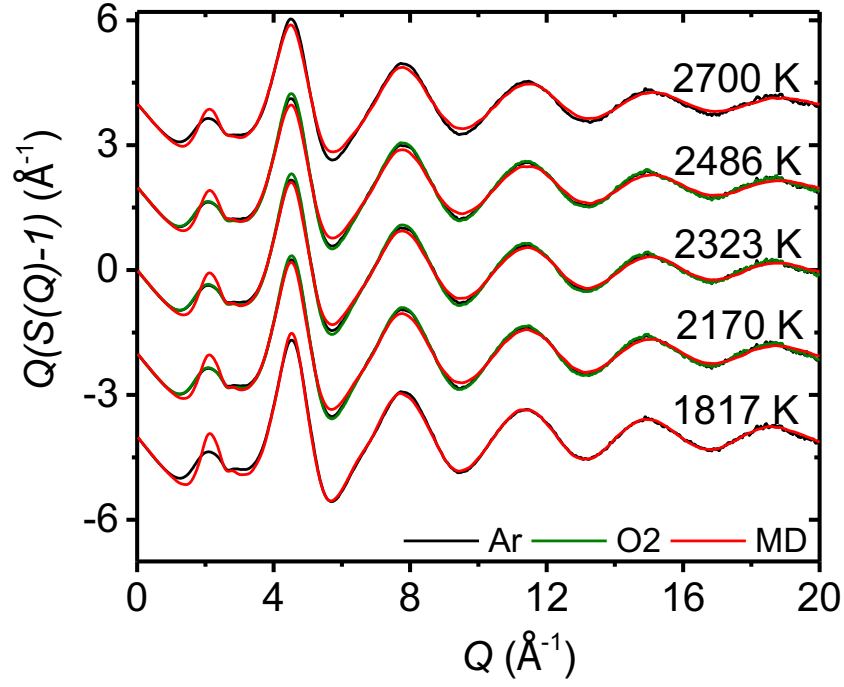


**Figure S1.** Comparison of  $Q \cdot [S(Q)-1]$  for liquid alumina in argon (black curve), in oxygen (green curve) and MD simulation (red) at different temperature. Vertical offsets have been applied for clarity.

**Figure S2** compares the EPSR of amorphous sample 1 with supercooled liquid at 1817 K. A density of  $0.0915 \text{ \AA}^3$  was used because of the best fitting result with the diffraction data. It is indicated that the main differences of amorphous and supercooled liquid are derived from the oxygen-related correlations Al-O and O-O.

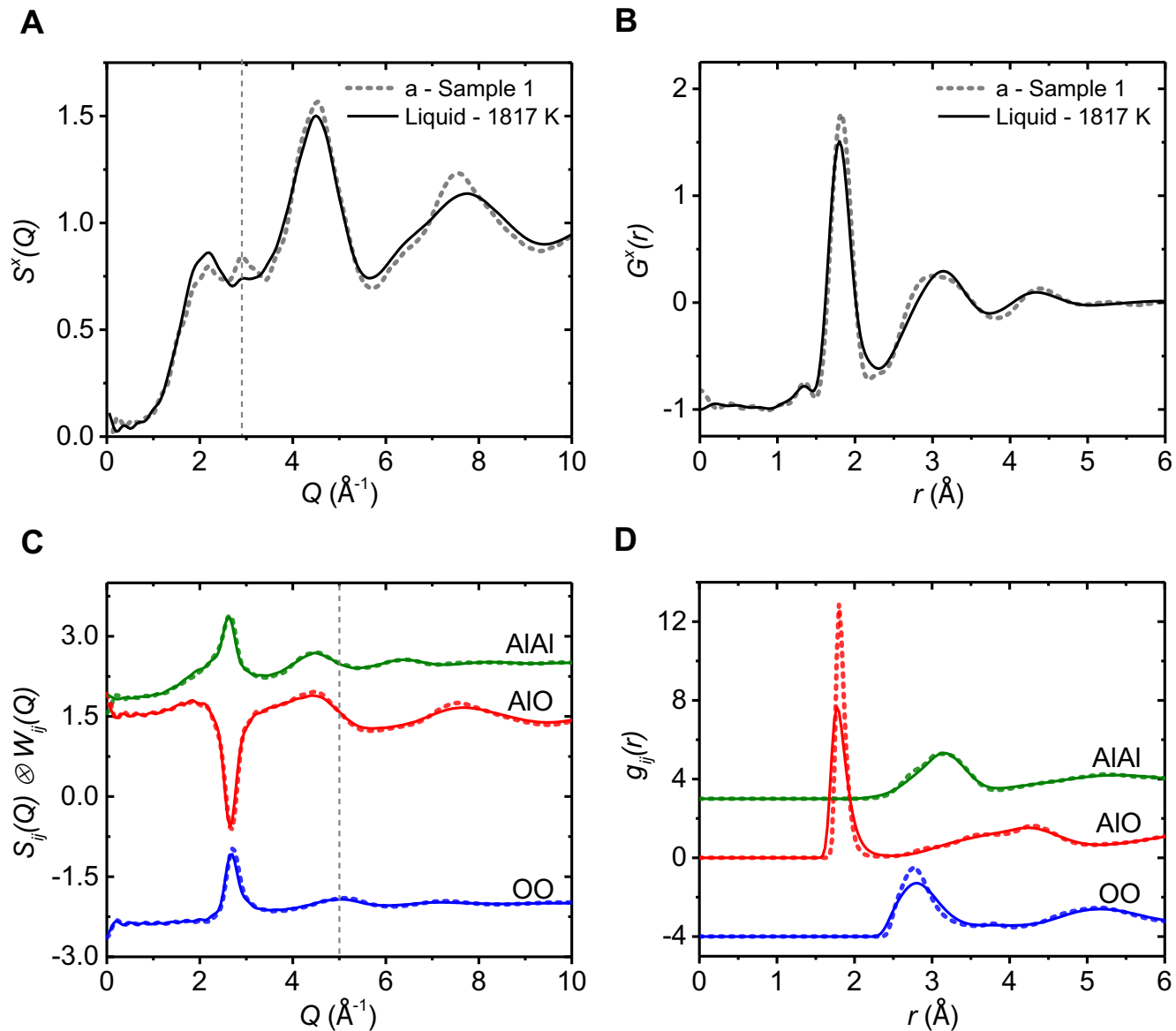


**Figure S2.** The total (A, B) and partial (C, D) x-ray structure factor  $S(Q)$  (A, C) and pair distribution function  $G(r)$  (B, D) from EPSR for amorphous sample 1 (solid line) with a density of  $0.0915 \text{ \AA}^3$ , and liquid at 1817 K (break line). Note that the  $S_{ij}(Q)$  in part (C) have been multiplied by the x-ray pair weighting factors,  $W_{ij}(Q)$ . Vertical offsets have been applied for clarity.

**Figure S3** plots the temperature dependence of the volume of crystalline corundum alumina obtained by MD simulation using Du and Corrales potential (Du and Corrales, 2007) with 5760 atoms. The melting point turns out to be 2800K, which is ~500K higher than the experimental value of 2327K (Schneider, 1970).

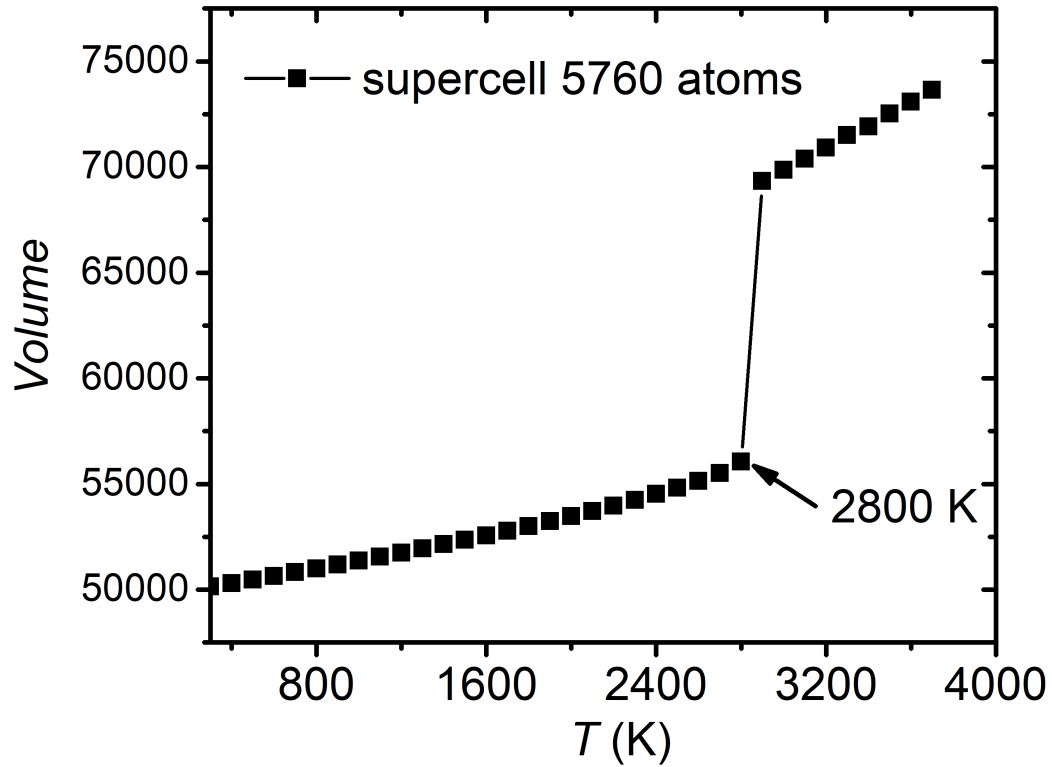


**Figure S3.** The temperature dependence of the volume of crystalline corundum alumina from MD simulation. The arrow indicates the estimated melting point from simulation.

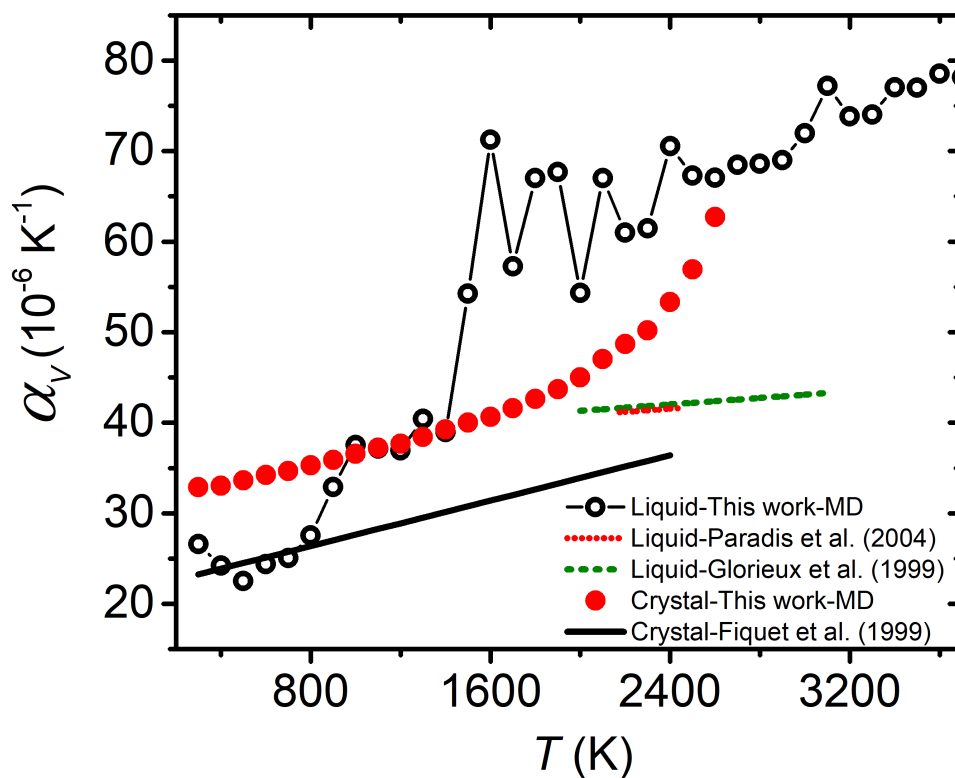


**Figure S4.** The temperature dependence of the volume thermal expansion coefficient  $\alpha_v$  of crystalline corundum and liquid alumina.

## References:

- Du, J., and Corrales, L. R. (2007). Understanding lanthanum aluminate glass structure by correlating molecular dynamics simulation results with neutron and X-ray scattering data. *J. Non-Cryst. Solids* 353, 210-214. doi: 10.1016/j.jnoncrysol.2006.06.025
- Schneider, S. J. (1970). Cooperative determination of the melting point of alumina. *Pure Appl. Chem.* 21, 115-122.